GEOPHYSICS, VOL. 68, NO. 4 (JULY-AUGUST 2003); P. 1224–1231, 10 FIGS.
10.1190/1.1598114

Real-time resistivity sounding using a hand-held broadband electromagnetic sensor

Haoping Huang* and I. J. Won*

ABSTRACT

Common situations encountered in geophysical investigations involving environmental and engineering problems call for simple and fast onsite interpretation of the survey data so results can be available in a timely manner for the projects. We have developed a method of interpreting broadband electromagnetic induction (EMI) data using a hand-held electromagnetic (EM) sensor based on a layered-earth model. In conductive environments, a hand-held EM sensor yields sufficient information for shallow resistivity soundings. The result is a conductivity–depth section based on the frequency-sounding principle. Tests using simulated data show that the method can reasonably recover earth conductivity structures with up to several layers.

We have field tested the method using data obtained with a GEM-2 broadband EMI sensor. The conductivity–depth section converted from the field data reasonably reflects the known variations in earth conductivity. Because the current GEM-2 is band-limited to 48 kHz, the method works mainly in conductive environments. Sample GEM-2 and GEM-3 data collected over shallow seawater produced a bathymetric section with a precision of a few centimeters. Application of the method in resistive environments requires a broader bandwidth.

INTRODUCTION

There are two common methods of active electromagnetic (EM) sounding. Depth sounding by changing the source–receiver separation is called geometrical sounding, which usually requires multiple operators tending various separations (or an array) connected to a central console by cables. Maintaining precise coil separation or orientation is difficult; therefore, some measurements (e.g., in-phase components) are often abandoned. The fieldwork is often slow and laborious, requiring heavy logistic support. Depth sounding by changing source frequency is called frequency sounding. This method involves fixed source–receiver geometry so the sensor may be built into a single rigid body that precisely maintains its geometry. A hand-held sensor that can measure, simultaneously and instantly, multiple frequency responses would provide tremendous advantages in speed, cost, and logistics.

The goal of depth sounding is to determine a 1D earth structure below a survey location. For a geometrical sounding, the location is the center of an expanding array. For a frequency sounding using a small sensor, it is the sensor location itself because the source and receiver are close together compared to the depth of investigation. The resolution decreases with depth because of either lateral averaging in geometrical sounding or with downward spreading of the source field in frequency sounding. Often, a 1D earth at each point is stitched along a survey line to render an approximate 2D conductivity profile. The basic data, however, can be used for full 2D or 3D inversion.

Making a small, broadband EM sensor, however, has posed significant technical challenges in two aspects: (1) primary field cancellation and (2) broadband operation. Because of the source–receiver proximity, the primary field at the receiver is strong and thus must be sufficiently reduced (or bucked) to accommodate a small secondary field. This requires precise coil design and placement. The broadband requirement is obvious in that the bandwidth must be as wide as possible to cover desired ranges in skin depth. However, operating a single set of coils in a broadband requires very advanced power-switching technology and high-speed, real-time digital electronics. Because of these technical difficulties, there have been few commercial broadband EM sensors until very recently.

The GEM-2 (Won et al., 1996), used for the examples in this paper, has a coil separation of 1.66 m and a bandwidth of a few hundred hertz to 48 kHz, about 2 to 3 decades in frequency. Portability is one of its main design criteria. Small coil separation coupled with a limited bandwidth can result in low induction number responses, particularly on a resistive earth where a given bandwidth may not produce sufficient frequency dependence for depth sounding. An argument on validity of a

Published on Geophysics Online January 30, 2003. Manuscript received by the Editor December 20, 2001; revised manuscript received December 2, 2002.
*Geophex, Ltd., 605 Mercury St., Raleigh, North Carolina 27603. E-mail: huang@geophex.com; ijwon@geophex.com.
© 2003 Society of Exploration Geophysicists. All rights reserved.

sensor with small coil separation solely based on the induction number, however, can be misleading. A small sensor can be used for depth sounding if it has (1) a sufficient sensitivity to resolve the small frequency dependence in a resistive area, (2) a large dynamic range to accommodate near-surface conductive effects, and (3) an ability to avoid certain frequencies with high noise levels caused by local sources such as power lines. A sensor that can meet these requirements can be used for depth sounding in a variety of geological settings. The GEM-2 has been designed to satisfy these requirements.

There are ample case histories that have used broadband EM data for characterizing landfills, pits and trenches, contaminant plumes, underground facilities, and many other applications (Won et al., 1996, 1997, and 1998; Keiswetter and Won, 1997; Keiswetter et al., 1997; Murray and Keiswetter, 1998; Witten and Calvert, 1999; Sternberg and Birken, 1999; Huang and Won, 2000). Interpretation is commonly based on the measured in-phase and quadrature components and mapping of apparent conductivity derived from the EM responses (Won et al., 1996 and 1997; Huang and Won, 2000). Often, EM data are converted to a 1D conductivity–depth section, as have been done by many researchers, e.g., Holladay et al., 1986; Paterson and Reford, 1986; Won and Smits, 1986; Hoekstra and Blohm, 1990; Huang and Palacky, 1991; Fitterman and Deszcz-pan, 1998; Sengpiel and Siemon, 1998, 2000.

The primary interest of this paper applies to environmental sites that have conductive plumes (e.g., brine contamination at oil wellheads) resulting in high induction numbers suitable for small sensors. In addition, the depth of interest is shallow in environmental investigations, commonly down to tens of meters. In such cases, frequency sounding using a small sensor by a single person is extremely fast and cheap, in comparison with geometrical sounding. We present a rapid frequency sounding method using a hand-held sensor to derive a 1D resistivity at each location, which may be stitched into a pseudo-2D profile. In all examples presented, we assume that the earth has the same permeability and permittivity as a vacuum.

JUSTIFICATON OF SMALL SENSOR SOUNDING

Figure 1 shows a coplanar coil pair at height h above a layered earth. Discussions on the forward and inverse problems for such a system appear in numerous publications. We use a damped least-squares inversion based on singular-value decomposition for solving the nonlinear inverse problem. A complete description of the forward and inverse problems is given by Huang and Fraser (2003). More details can be found in Ward and Hohmann (1988), Menke (1984), and Lawson and Hanson (1974).

The EM response is the in-phase (I) and quadrature (Q) components of the secondary magnetic field at each frequency, given the conductivity and thickness of each layer. Figure 2 shows the response of the GEM-2 sensor over a half-space as a function of induction number $\theta = (i\omega\sigma\mu/2)^{1/2}s$, where ω is the angular frequency, σ is the conductivity, μ is the magnetic permeability, and s is the coil separation. The low induction number range for a layered earth is defined as $\theta \leq 0.02$, where θ is the induction number in any of the layers (Spies and Frischknecht, 1991). The EM response in this range is small and of little frequency dependence, which renders frequency sounding impractical. When $\theta \gg 1$, I reaches its highest value and Q goes to zero, which also makes the sounding impractical because no EM energy penetrates the earth. Therefore, a successful EM sounder should operate at a moderate induction number. For the GEM-2 with its coil separation of 1.66 m and an upper frequency limit of 48 kHz, many geological formations fall into a low to middle induction number where both I and Q have high intensity and strong frequency dependence. Figure 2 illustrates an induction number zone covered by a 1- to 48-kHz bandwidth over a 5-ohm-m (conductivity = 0.2 S/m) earth, which is not uncommon for environmental sites. As can be seen, the sensor covers a low to middle induction number zone where both I and Q are strong and frequency dependent, testifying that a small sensor can be used for soundings in such environments. In practice, the environmental noise level, which is site dependent and is always higher than the instrument noise level, governs ultimate utility of the sensor.

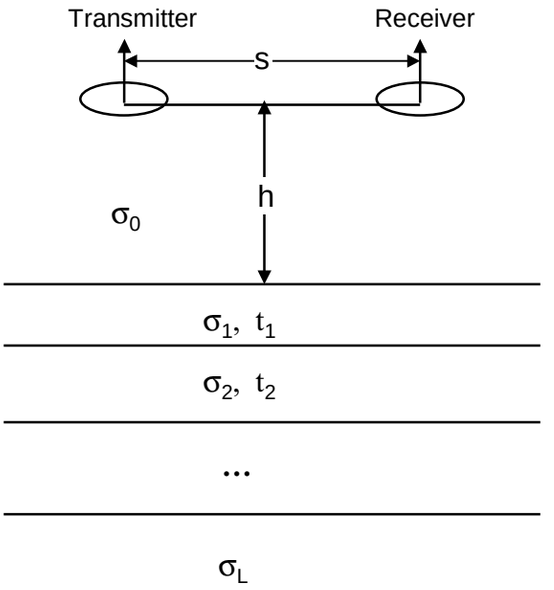

FIG. 1. Geometry of the EM sensor over a layered earth, where σ is the conductivity, t is the thickness of each layer, the subscripts stand for number of layers, s is the coil separation, and h is the sensor height.

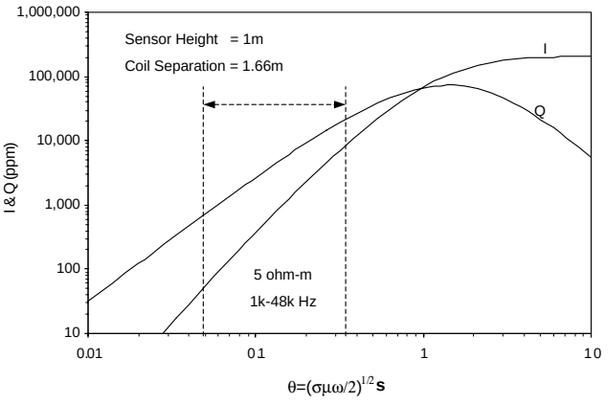

FIG. 2. The in-phase and quadrature responses as a function of induction number $\theta = (\sigma\mu\omega/2)^{1/2}$s.

MODELS IN ENVIRONMENTAL AND ENGINEERING GEOPHYSICS

Targets in environmental and engineering geophysics can be grouped into three shape categories: (1) isolated objects such as unexploded ordnance and drums, (2) long linear objects such as pipes and trenches, and (3) sheetlike objects with large horizontal extent such as high-salinity soils and contaminated groundwater. The first two categories must be modeled in two or three dimensions, while the third can often be modeled in one dimension, which is suitable for sounding. The earth can be viewed as one dimensional as long as its structure does not change much within the sensing volume. In such cases, adjacent 1D soundings may be stitched to render a pseudo 2D cross-section. Such practices are quite common in many other geophysical soundings. For example, Sengpiel and Siemon (1998) show examples of 1D multifrequency inversion from 3D resistivity distributions and find they provide useful results even in the presence of lateral changes. Similar conclusions come from Sattel (1998) in his 1D inversion using time-domain airborne data. Such 1D approximations may break down where the earth is highly heterogeneous with, for instance, isolated bodies and steeply dipping layers (Ellis, 1998). However, such heterogeneities, are easily recognized by inspecting the EM data set.

Many geologic features in Figure 3 may be approximated by a stitched 1D earth having two layers. Figure 3a, for instance, shows a simple case of resistive bedrock below a conductive overburden, while Figure 3b may be applicable to a conductive basement below resistive overburden—say, because of inorganic contamination—for which we can determine the depth to the basement. Ice-over-seawater and seawater-over-sediment are other two-layer examples with strong conductivity contrasts which can be resolved easily from broadband EM data spanning the appropriate frequency range.

Figure 3 also includes several cases for which a three-layer model would be more suitable. For example, as inorganic contaminant is confined within a layer sandwiched between two other layers, a three-layer model may be used to estimate its depth and thickness. The model could apply to oil fields with brine contamination and to salt evaporation fields where brines may have migrated and contaminated groundwater. A three-layer model can be used to evaluate the extent and pathways of contaminants. In addition, coastal hydrology may be approximated by a three-layer model; the freshwater–saltwater interface and saltwater extent can be estimated from the EM sounding data. More layers may be necessary to study some complicated situations. EM sounding would also be useful for studying coastal aquifers where saltwater has intruded because of excessive pumping (e.g., Hoekstra and Blohm, 1990).

In practice, we collect broadband EM data at a location along a profile that may be part of a larger areal survey. For instance, the GEM-2 allows data collection using simultaneous, multiple frequencies (as many as 10), which takes less than 1 s to acquire at each location. To concentrate power in each frequency, the GEM-2 steps between frequencies—one frequency at a time, each lasting one-thirtieth of a second—for as many steps as desired. Since the sensor also has a real-time downloading capability, a PC connected to the sensor can rapidly process the field data, display the inversion result, and compile it into a profile or depth-slice map. The time required at each data point can be very short, so continuous profiling is possible at a walking speed.

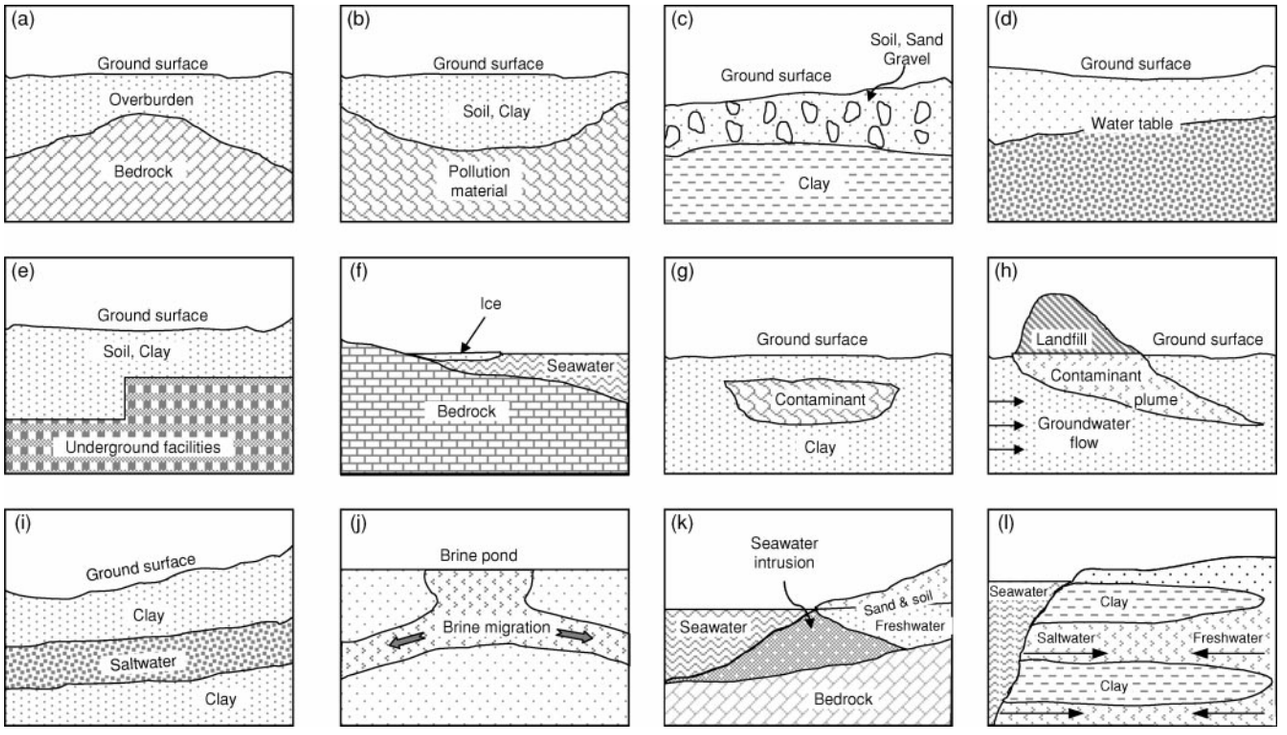

FIG. 3. Geologic models encountered in common environmental and engineering problems.

SYNTHETIC DATA EXAMPLES

We first tested the inversion algorithm using 10-frequency synthetic responses in a range from 90 Hz to 48 kHz with a sensor height of 1 m and a transmitting–receiving coil separation of 1.66 m (for GEM-2). Obviously, the noise level depends on the background EM environments. In this study, we added up to 20% random noise to the synthetic responses, which we consider realistic from our experience with the GEM-2 in urban sites.

The first example uses a two-layer model to simulate a moderately resistive overburden over a conductive basement. The overburden has a resistivity of 50 ohm-m and a thickness of 10 m, while the basement has a resistivity of 5 ohm-m.

Figure 4a shows the model and computed in-phase and quadrature responses at 10 frequencies. Figure 4b presents the inverted model without noise (solid line) and with 20% random noise (dotted line). The starting values for resistivity are determined using the apparent resistivity algorithm of Huang and Won (2000), and the starting thicknesses are from an effective depth algorithm similar to that of Huang and Fraser (1996). For example, the starting values for resistivity are 39 ohm-m for the upper layer, 12 ohm-m for the basement, and 5 m for the upper-layer thickness. As can be seen, the noise-free simulated responses recover the model exactly, while for the noisy simulated data, the depth is overestimated by about 12% along with a slightly underestimated basement resistivity. Figure 4c presents the decrease in the relative fitting error normalized against the starting misfit. For the no-noise case, the misfit is reduced by more than eight orders of magnitude in twelve iterations, while for the noisy case, the improvement stops at about the fourth iteration.

Figures 4d–e show composite profiles based on inversion results for the same model in Figure 4a but with varying depth, from 1 to 50 m, to the basement. The somewhat optimistic thickness of 50 m is used to investigate theoretical resolution power of a small EM sensor. Figure 4d is the profile from the noise-free case, and Figure 4e is from the 20% noisy synthetics. The depth to the lower layer increases linearly from 1 m on the left to 50 m on the right.

Next, we consider a two-layer model that is the same as in Figure 4a but with its resistivities reversed—an example of conductive overburden and a difficult case. Figure 5 shows the corresponding results. All model parameters are well resolved for the noise-free responses but are not for the noisy responses.

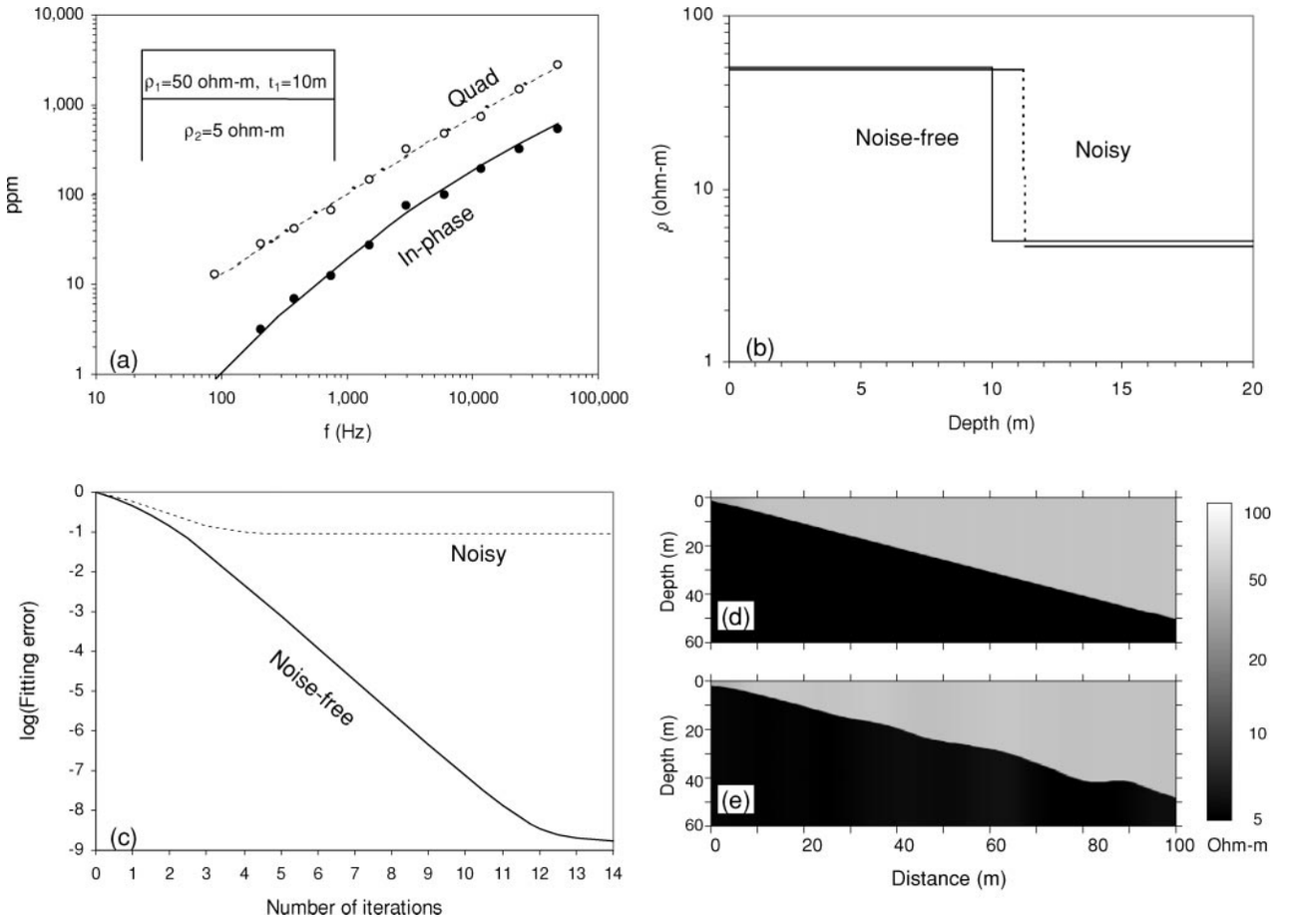

FIG. 4. (a) A two-layer model and simulated EM responses. Solid and dotted lines are noise free, and the circles are with 20% noise. (b) The inverted models: solid line—no noise; dashed line—noise added. (c) Fitting error as a function of iterations. Depth sections recovered from (d) noise-free case and (e) 20%-noise case. In (d) and (e), the true model parameters are the same as those in (a) except for thickness that linearly varies from 1 to 50 m.

Particularly when the upper-layer thickness is greater than 35 m, it is significantly underestimated, and the basement resistivity is underestimated as well. While the basement resistivity is poorly resolved, its boundary is clearly defined, particularly at shallow depths.

Random noise may be mitigated by stacking the data over time. Figure 6 shows a three-layer model for which we collect sixty 2-s long data points, each having a 20% instantaneous random noise. By stacking 60 times, the random noise should decrease by $1/\sqrt{60}$ or 2.6%, resulting in a significant improvement as shown in Figures 6e and 6f. Figure 6f is the inversion result from noisy responses without stacking.

FIELD EXAMPLES

The first two examples show seawater depth sounding using data from GEM-2 or GEM-3 (Won et al., 1996, 1997) at a beach near Wilmington, North Carolina. We collected the data by wading from a water depth of 0 to 75 cm while holding the sensor about 1 m above the water. Six frequencies were used, ranging from 2 to 20 kHz. EM data and inversion results are shown in Figure 7 for GEM-2 and Figure 8 for GEM-3. Figures 7a,b and 8a,b show the in-phase and quadrature data, while Figures 7c and 8c are the inversion results based on a two-layer model. Typical seawater resistivity in middle latitudes is 0.25 ohm-m (Won and Smits, 1986), which leaves the water depth and sea-floor resistivity to be determined. The results are displayed in Figures 7c and 8c; both GEM-2 and GEM-3 results agree, within a measurement error of 5%, with the water depths as determined with a ruler.

The next field example is from a mirror manufacturing plant. Some years ago, broken mirror pieces, also known as cullet, were stored above ground in a huge pile and, consequently buried on site. Subsequent site renovation that included paving completely concealed the burial site. The cullet contained a lead-based compound that eventually leached into groundwater, causing lead contamination. A GEM-2 survey, using frequencies of 4050 Hz and 12270 Hz, located the buried cullet and identified preferred drilling and chemical sampling locations (Huang and Won, 2000).

The inversion algorithm was tested on data from a portion of a survey line across the buried cullet (see Figure 9a). The purpose was to estimate depth to the buried cullet materials and possibly its vertical extent. Figure 9b shows two-layer inversion results as a resistivity–depth section. Resistivity lows (or conductivity highs) in the middle of the section reflect the buried cullet material, which is located at a depth of about 3.5 m. True depths to the cullet material range from 1 to 4.5 m. Next, we used a three-layer model to determine the cullet thickness (Figure 9c), which appears to be unstable and generally greater

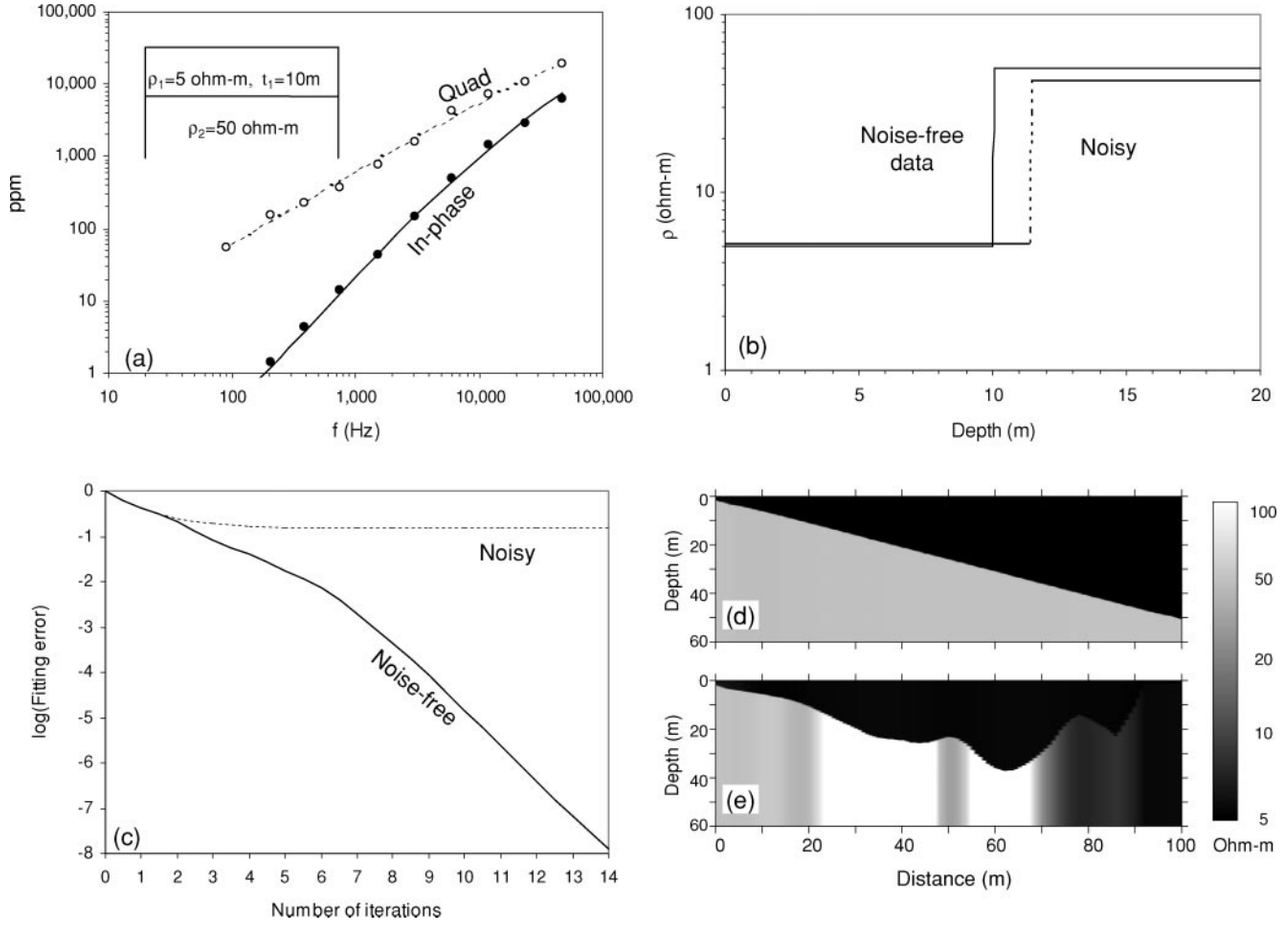

FIG. 5. Same as Figure 4 except for resistivities that are reversed between the two layers.

than 10 m. This thickness may be an overestimate, particularly because it exceeds the skin depth of the cullet, which is 7 m at 4050 Hz for the cullet resistivity.

The last field example is from Hutchinson, Kansas, where the Kansas Geological Survey conducted an EM survey using a GEM-2. This survey was part of an effort to locate abandoned brine wells. The survey verified most of the EM anomalies, including an abandoned uncapped brine wellhead, the main purpose of the survey (Xia, 2001). The wellhead, used for solution mining of salt, had released a mixture of natural gas and saltwater that polluted the groundwater. The groundwater, the water supply for the city of Hutchinson, is from a Quaternary alluvium of sands and gravels having a thickness of 15 m (50 ft) or more and has been reported to have a chloride concentration as high as 44 g/liter, which is about 25% higher than that of seawater. The formation resistivity derived from the EM data may be displayed either as cross-sections or as maps, which would outline the brine contamination, freshwater–saltwater interface, and brine thickness. Correlations between formation resistivity and salt content can be established based on the resistivity and well-log data. Thus, resistivity maps can be used as water

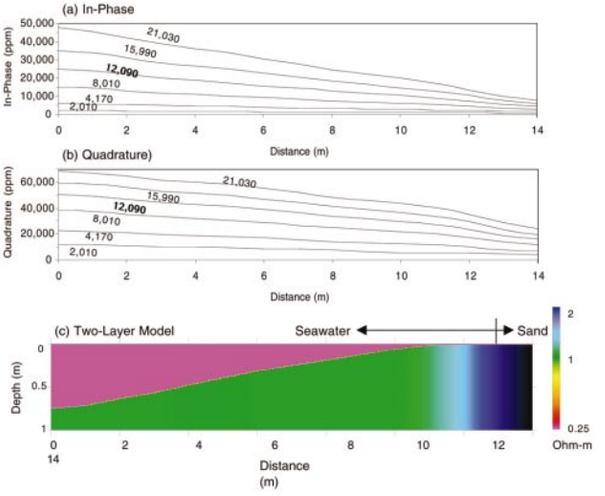

FIG. 7. GEM-2 data obtained from a beach, (a) in phase and (b) quadrature. Depth section (c) is based on 1D inversion using a two-layer model.

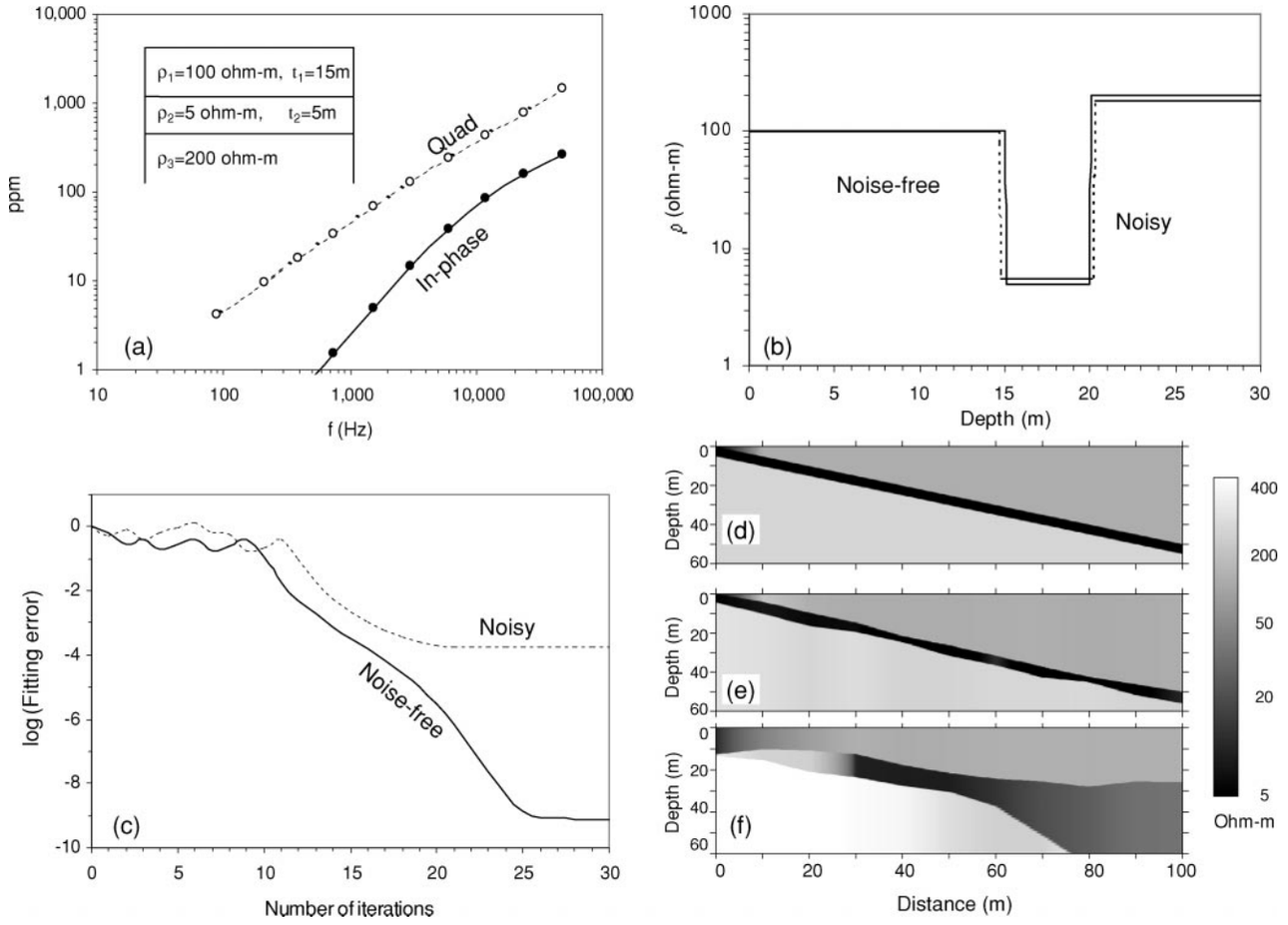

FIG. 6. (a) A three-layer model and EM data. Solid and dotted lines are noise free, and the circles are with 20% noise but stacked 60 times. (b) The inverted models: solid line—no noise; dashed line—noise added. (c) Fitting error as a function of iterations. Depth sections recovered from (d) noise-free case, (e) 20% noise with stacking, and (f) 20% noise without stacking. In (d), (e), and (f), the true model parameters are the same as those in (a) except for thickness of the upper layer that varies from 1 to 50 m.

quality maps with better coverage than is possible from well samples alone.

The example shown here is from an area approximately 930 m^2 (10000 ft^2) large with data collected at three frequencies—2430, 7290, and 18270 Hz—and line spacing of 0.61 m (2 ft). Figures 10a–d show GEM-2 data and interpreted resistivity sections from two survey lines. A thin conductive layer (purple–red–orange) near the surface appears on both sections, which is interpreted to be the brine layer with a resistivity of less than 10 ohm-m. The lower layer shows resistivities greater than several tens of ohmmeters, indicating freshwater. The 1D model breaks down on highly heterogeneous structures as implied—for instance, at 13 m and 25 m of line 86. As a further example, Figure 10e shows the depth-slice maps at 1, 2, 3, and 5 m. This 3D rendering indicates that brine concentrates in the southwest at depths of 1 or 2 m and becomes deeper to the northwest.

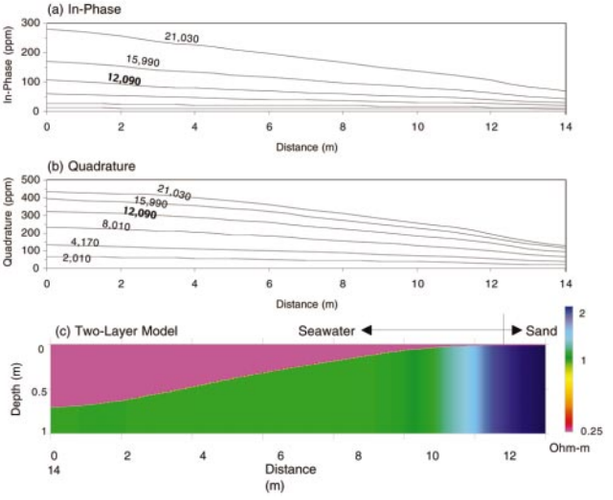

FIG. 8. GEM-3 data obtained from a beach, (a) in phase, and (b) quadrature. Depth section (c) is based on 1D inversion using a two-layer model.

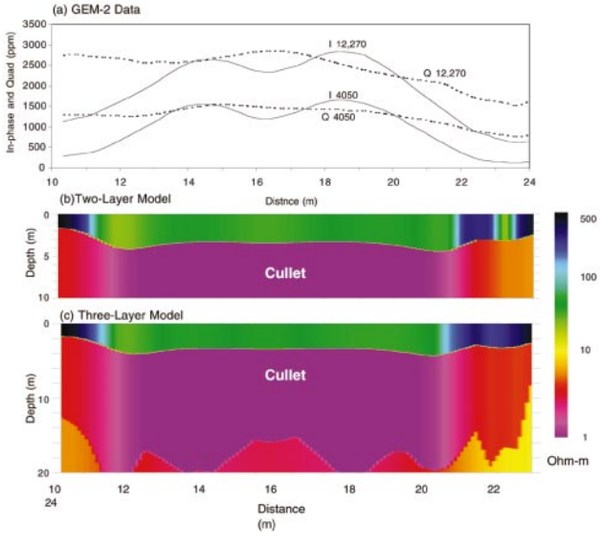

FIG. 9. (a) GEM-2 data from an old mirror manufacturing plant. Solid curves are for in phase, dashed curves for quadrature. The depth sections are based on 1D inversion using (b) two-layer and (c) three-layer models.

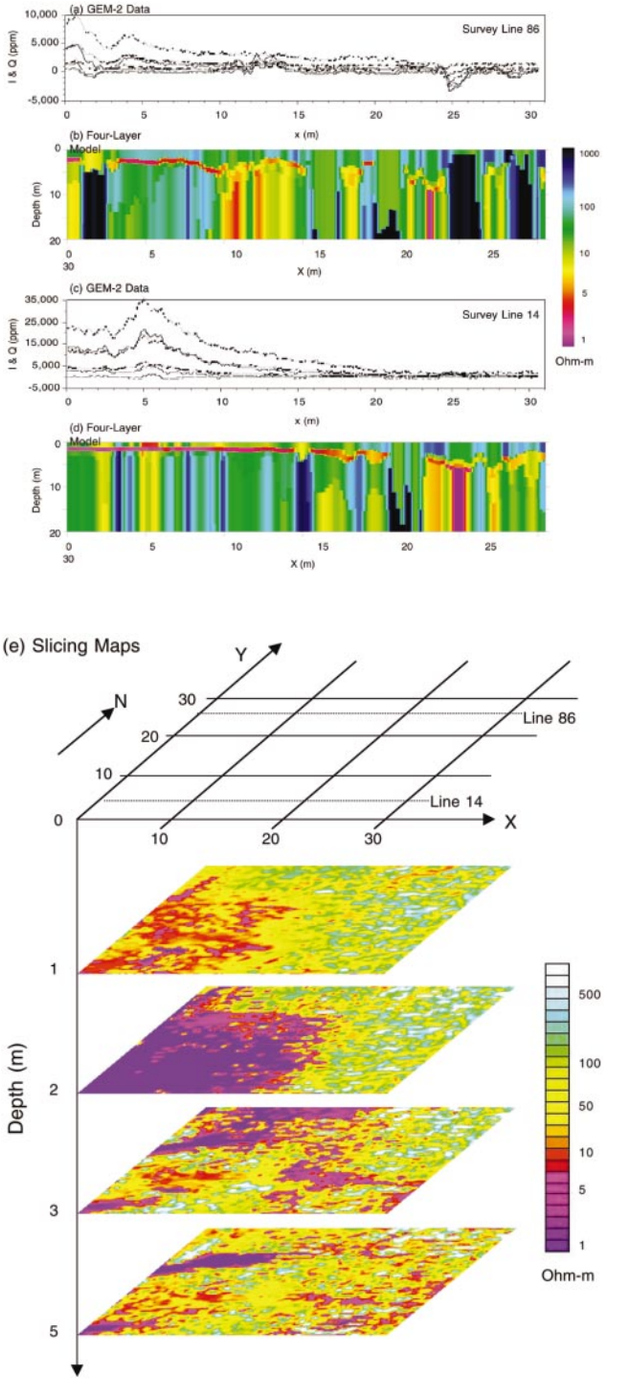

FIG. 10. Two GEM-2 profiles, (a) and (c), from a survey in Hutchinson, Kansas. The solid curves stand for in phase, and the dashed lines are the quadrature at 18 270, 7290, and 2430 Hz. The depth sections (b) and (d) are based on 1D inversion using a four-layer model. Resistivity slice maps (e) at depths of 1, 2, 3, and 5 m.

CONCLUSIONS

Many situations encountered in environmental and engineering geology can be simplified as a layered-earth model. We have developed an inversion algorithm for interpreting broadband EM data obtained using a hand-held EM sensor, which is able to gain information on shallow geoelectric structures in conductive environments. The information is interpreted based on a layered-earth model, yielding the resistivity and thickness of each layer for a layered earth. Simulations show that the method can reasonably recover a simple two- or three-layer earth.

This approach has been tested using field data obtained with GEM-2 and GEM-3 broadband EMI sensors. The resistivity–depth section converted from the broadband data reasonably reflects the known variations in earth resistivity, as shown in field examples. The inversion is relatively robust and works best in conductive environments because of the limited bandwidth of currently available sensors. For instance, the GEM-2 data collected over shallow seawater produced a bathymetric section with a precision of a few centimeters. As a result of the bandwidth limitation, our method is useful mainly for sounding shallow earth in a conductive environment. In moderately conductive areas—say, with resistivity ranging from 10 to 30 ohm-m—we recommend higher frequencies and a two- or three-layer model.

REFERENCES

Ellis, R. G., 1998, Inversion of airborne electromagnetic data: Expl. Geophys., **29**, 21–27.

Fitterman, D. V., and Deszcz-pan, M., 1998, Helicopter EM mapping of saltwater intrusion in Everglades National Park, Florida: Expl. Geophys., **29** 240–243.

Hoekstra, P., and Blohm, M. W., 1990, Case histories of time-domain electromagnetic soundings in environmental geophysics, *in* Ward, S. H., ed., Investigations in Geophysics No. 5: Geotechnical and Environmental Geophysics, 1-15.

Holladay, S. J., Valleau, N., and Morrison, E., 1986, Application of multifrequency helicopter electromagnetic survey to mapping of sea-ice thickness and shallow-water bathymetry, *in* Palacky, G. J., Ed., Airborne resistivity mapping: Geol. Surv. Canada, 91–98.

Huang, H., and Fraser, D. C., 1996, The differential parameter method for multifrequency airborne resistivity mapping: Geophysics, **61**, 100–109.

———2003, Inversion of helicopter electromagnetic data to a magnetic conductive layered earth: Geophysics, **68**, 1211–1223, this issue.

Huang, H., and Palacky, G. J., 1991, Damped least-squares inversion of time-domain airborne EM data based on singular value decomposition: Geophys. Prosp., **39**, 827–844.

Huang, H., and Won, I. J., 2000, Conductivity and susceptibility mapping using broadband electromagnetic sensors: J. Environ. Eng. Geophys., **5**, No. 4, 31–41.

Keiswetter, D. A., and Won, I. J., 1997, Multifrequency electromagnetic signature of the cloud chamber, Nevada test site: J. Environ. Eng. Geophys., **2**, No. 2, 99–104.

Keiswetter, D., Novikova, E., Won, I. J., Hall, T., and Hanson, D., 1997, Development of a monostatic, multifrequency electromagnetic mine detector: Soc. Optical Eng., **3079**, 831–839.

Lawson, C. L., and Hanson, R. J., 1974, Solving least-squares problems: Prentice Hall, Inc.

Menke, W., 1984, Geophysical data analysis—Discrete inverse theory: Academic Press, Inc.

Murray, C., and Keiswetter, D., 1998, Application of magnetic and multi-frequency EM techniques for landfill investigations: Case histories: Symp. on Appl. Geophys. to Eng. and Environ. Problems, proceedings, 445–452.

Paterson, N. R., and Reford, S. W., 1986, Inversion of airborne electromagnetic data for overburden mapping and groundwater exploration, *in* Palacky, G. J., Ed., Airborne resistivity mapping: Geol. Surv. Canada, 39–48.

Sattel, D., 1998, Conductivity information in three dimensions: Expl. Geophys., **29**, 157–162.

Sengpiel, K. P., and Siemon, B., 1998, Examples of 1-D inversion of multifrequency HEM data from 3-D resistivity distributions: Expl. Geophys., **29**, 133–141.

———2000, Advanced inversion methods for airborne electromagnetic exploration: Geophysics, **65**, 1983–1992.

Spies, R. B., and Frischknecht, C. F., 1991, Electromagnetic sounding, *in* Nabighian, M. N., Ed., Electromagnetic methods in applied geophysics **2**: Soc. Expl. Geophys., 285–425.

Sternberg, B. K., and Birken, R. A., 1999, A new method of subsurface imaging—The LASI high frequency ellipticity system: Part 3—System tests and field surveys: J. Environ. Eng. Geophys., **4**, No. 4, 227–240.

Ward, S. H., and Hohmann, G. W., 1988, Electromagnetic theory for geophysical applications, *in* Nabighian, M. N., Ed., Electromagnetic methods in applied geophysics **1**: Soc. Expl. Geophys., 130–311.

Witten, A. J., and Calvert, G., 1999, Characterizing the distribution of near-surface solution channels using electromagnetic induction and ground penetrating radar: J. Environ. Eng. Geophys., **4**, No. 1, 35–43.

Won, I. J., and Smits, K., 1986, Application of the airborne electromagnetic method for bathymetric charting in shallow oceans, *in* Palacky, G. J., Ed., Airborne resistivity mapping: Geol. Surv. Canada, 99–106.

Won, I. J., Keiswetter, D., Fields, G., and Sutton, L., 1996, GEM-2: A new multifrequency electromagnetic sensor: J. Environ. Eng. Geophys., **1**, No. 2, 129–137.

Won, I. J., Keiswetter, D., Hanson, D., Novikova, E., and Hall, T., 1997, GEM-3: A monostatic broadband electromagnetic induction sensor: J. Environ. Eng. Geophys., **2**, No. 1, 53–64.

Won, I. J., Keiswetter, D., and Novikova, E., 1998, Electromagnetic induction spectroscopy: J. Environ. Eng. Geophys., **3**, No. 1, 27–40.

Xia, J., 2001, Feasibility study on using the electromagnetic method to locate abandoned brine wells in Hutchinson, Kansas: Kansas Geological Survey Open-File Report 2001-10.